SECTION -B-

THE USE OF PORPHYROBLASTS TO RESOLVE THE HISTORY OF MACRO-SCALE

STRUCTURES: AN EXAMPLE FROM THE ROBERTSON RIVER METAMORPHICS, NORTH

EASTERN AUSTRALIA

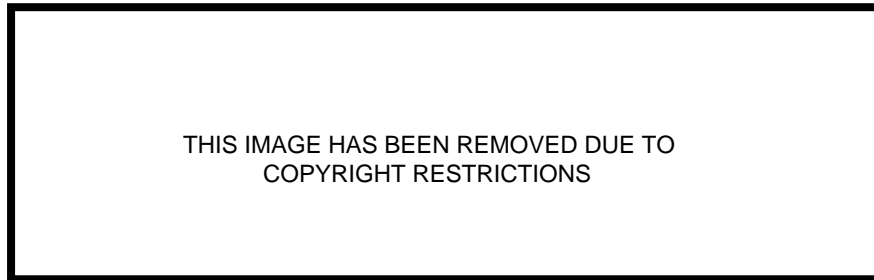THIS IMAGE HAS BEEN REMOVED DUE TO
COPYRIGHT RESTRICTIONS

Figure 1. Location map showing the major regional geological features of the central Georgetown Inlier, North Queensland, Australia. The inset box highlights the area in which detailed study was performed (Compiled from Withnall, 1985 and Bain et al., 1985).

THIS IMAGE HAS BEEN REMOVED DUE TO
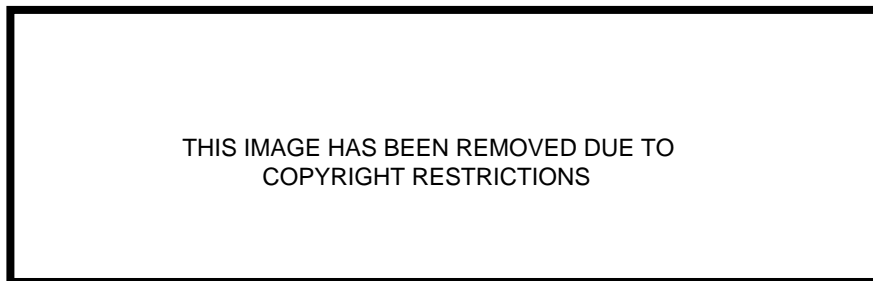COPYRIGHT RESTRICTIONS

Figure 2. Detailed geological map of the study area outlined in Fig. 1c

(modified from Bain et al., 1985). The folded dash lines, which crosscut the

lithologic trends, represent the sillimanite (sill), staurolite-andalusite (st-and),

chloritoid (cld) isograds. A-A` line shows the position of the cross-section in
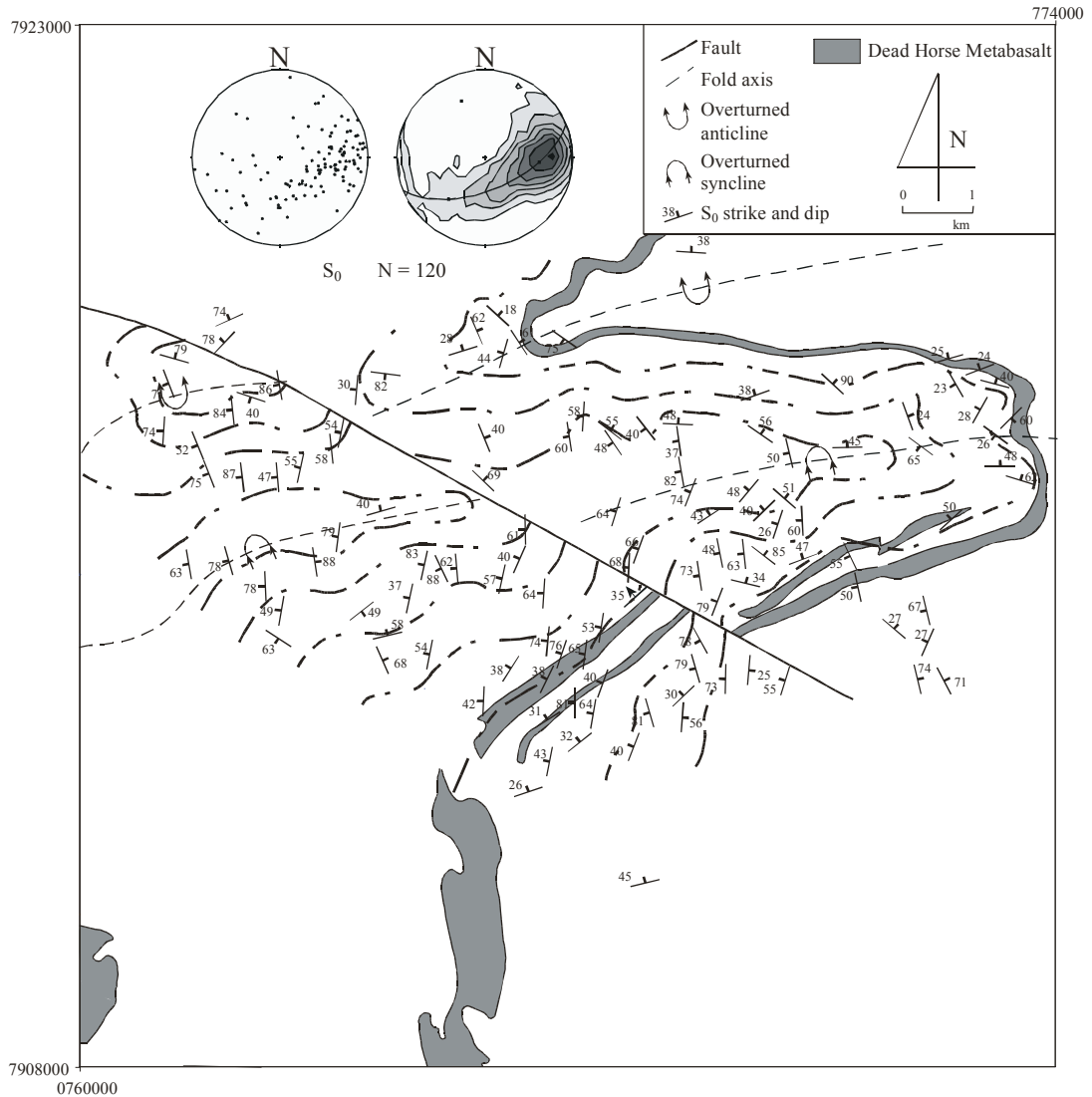
Fig. 12.

Figure 3. A structural map of bedding (S_0) orientations and form-line trends. Note, that in plan view, form lines lie parallel to the limbs of macroscopic folds outlined by the Dead Horse Metabasalt. Although these folds have ~E-W axial traces, stereonet plots suggest that S_0 is folded around NNW-SSE trending axes.

Figure 4. Photomicrograph from a vertical thin section shows garnet (grt) wrapped by a staurolite (st) porphyroblast (a). As shown in interpreted line diagram (b), two pre-matrix foliations were overgrown by garnet porphyroblast whereas staurolite porphyroblast overgrew S_1 and $S_{1/2}$ as represented by a crenulation hinge and the dominant matrix foliation in the matrix respectively. S_3 is a weak crenulation.
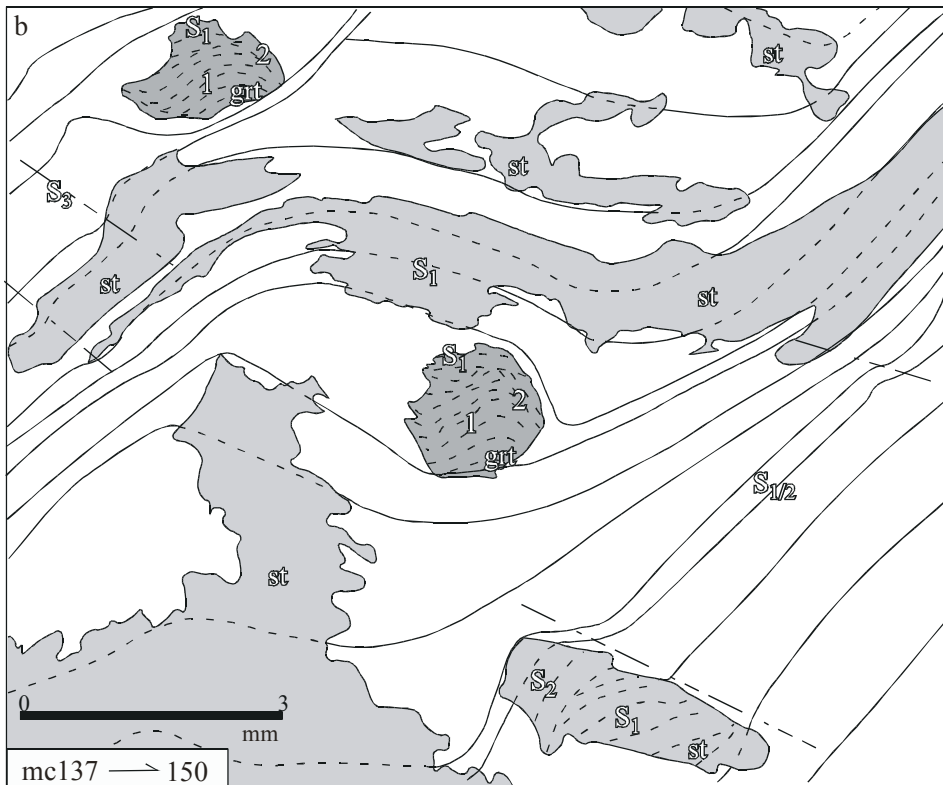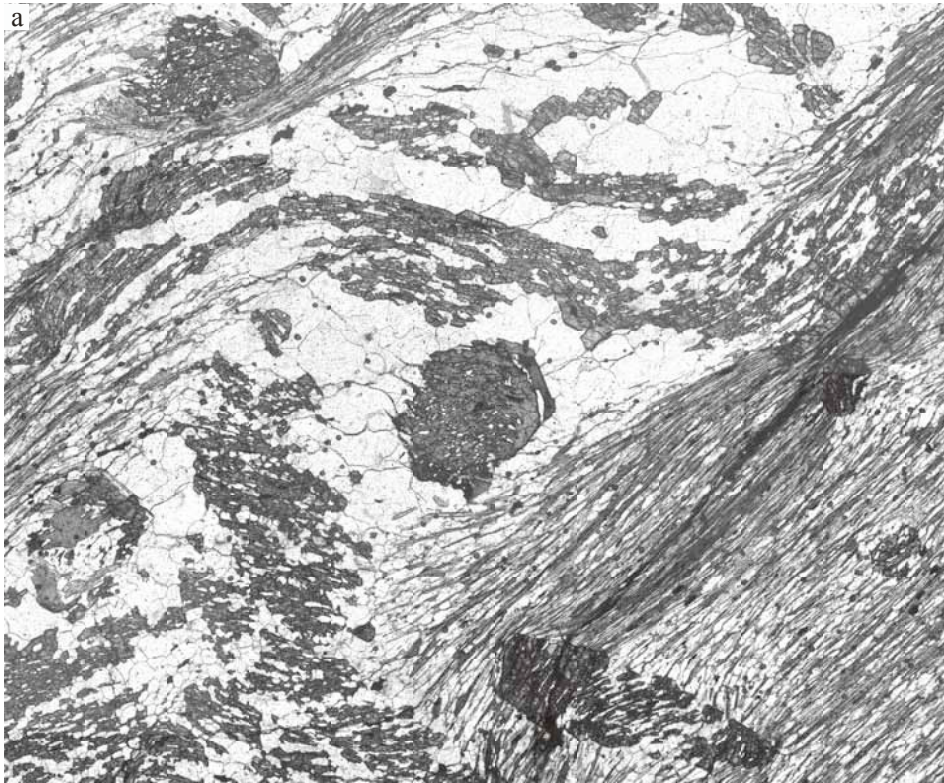
Figure 5. Photomicrograph from a vertical thin section shows a staurolite porphyroblast with sigmoidal type inclusions (a). Interpreted line diagram depicts the reactivation of the earlier foliation (S_1) in the matrix (b). S_1 is trapped within the staurolite as a hinge of a differentiated crenulation cleavage (S_2). Light barbed arrows represent the clockwise sense of shear on the steep S_2 foliation formed at the beginning of D_2. D_2 Q-domain (shaded with light grey) was destroyed in the matrix with anticlockwise shear sense (black barbed arrows) and S_1 was decrenulated and rotated to form a composite schistosity ($S_{1/2}$).
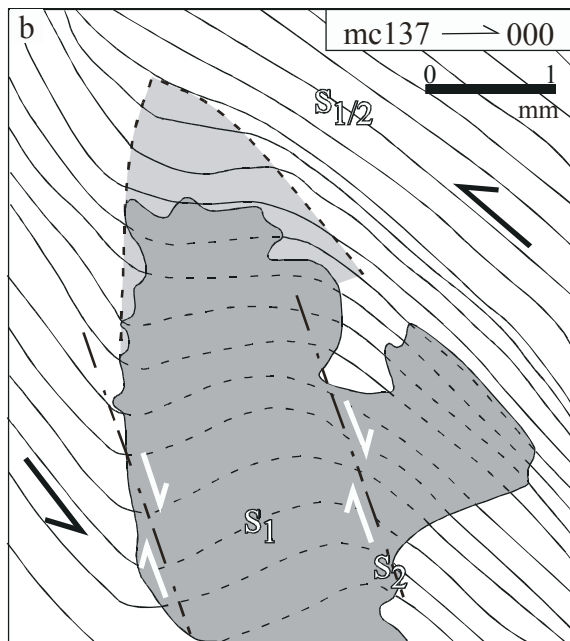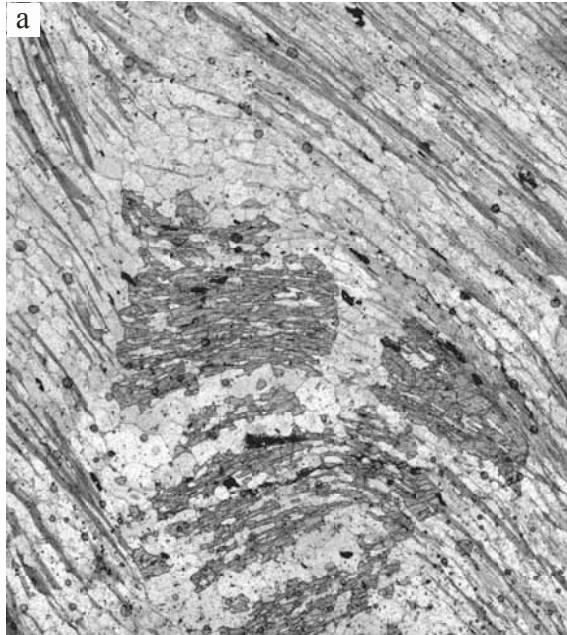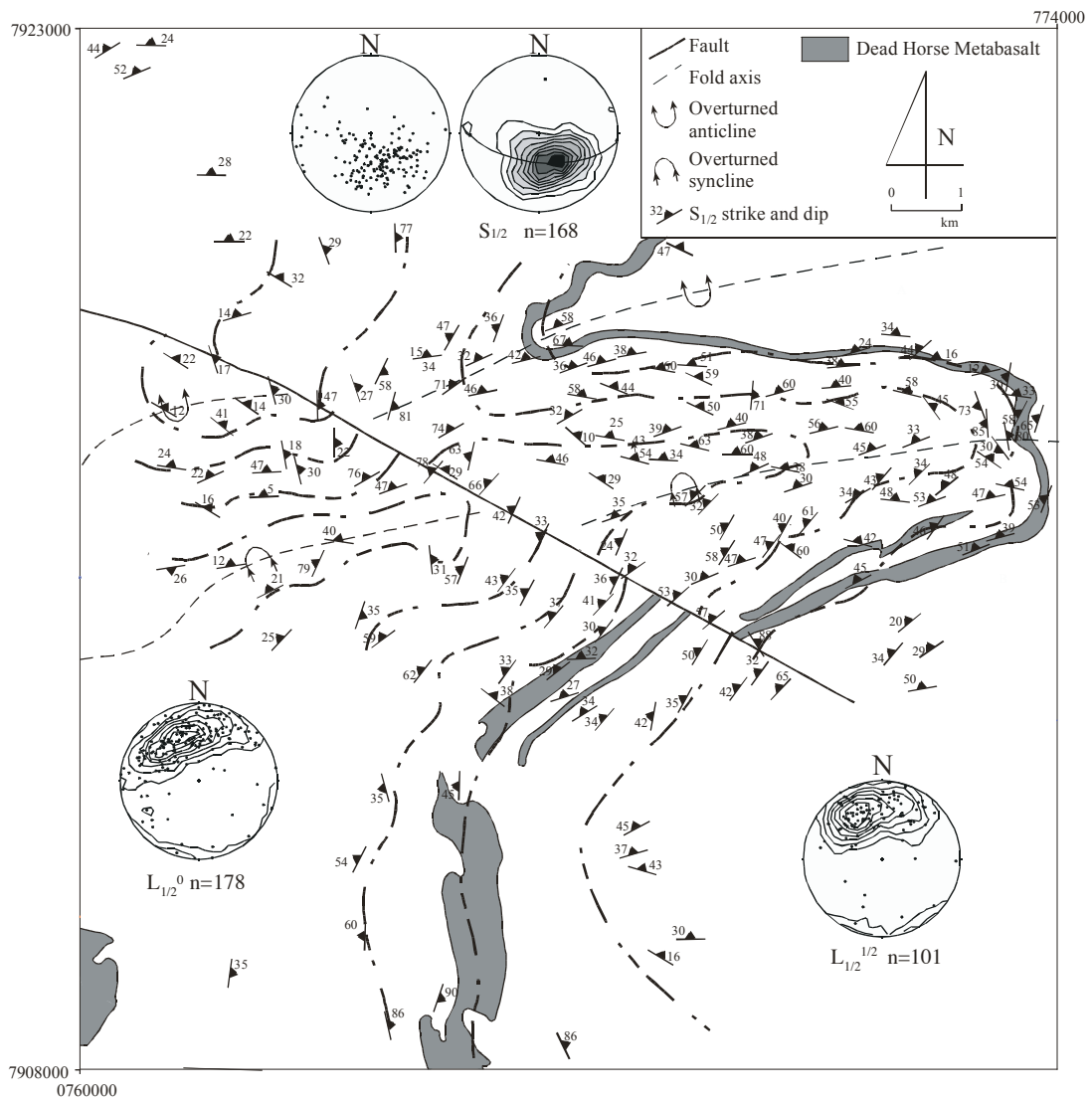
Figure 6. A structural map of the $S_{1/2}$ dominant foliation and interpreted $S_{1/2}$ form-lines. A stereonet plot of $S_{1/2}$ suggests folding around N-S axes. Stereonet plots of stretching lineations ($L_{1/2}^{1/2}$) and intersection lineations ($L_{1/2}^{0}$) indicate the distribution of these on the limbs of N-S folds (F_3).

Figure 7. Photomicrograph from a vertical thin section shows a garnet porphyroblast with a complex inclusion pattern (a). A line diagram shows the interpretation of successively formed foliations and textural discontinuities both in the porphyroblast and in the matrix (b). The numbers, 1-4 represents different groups of pre-existing foliations trapped within the porphyroblast. S_2-S_4 represents the foliations identified in the matrix.
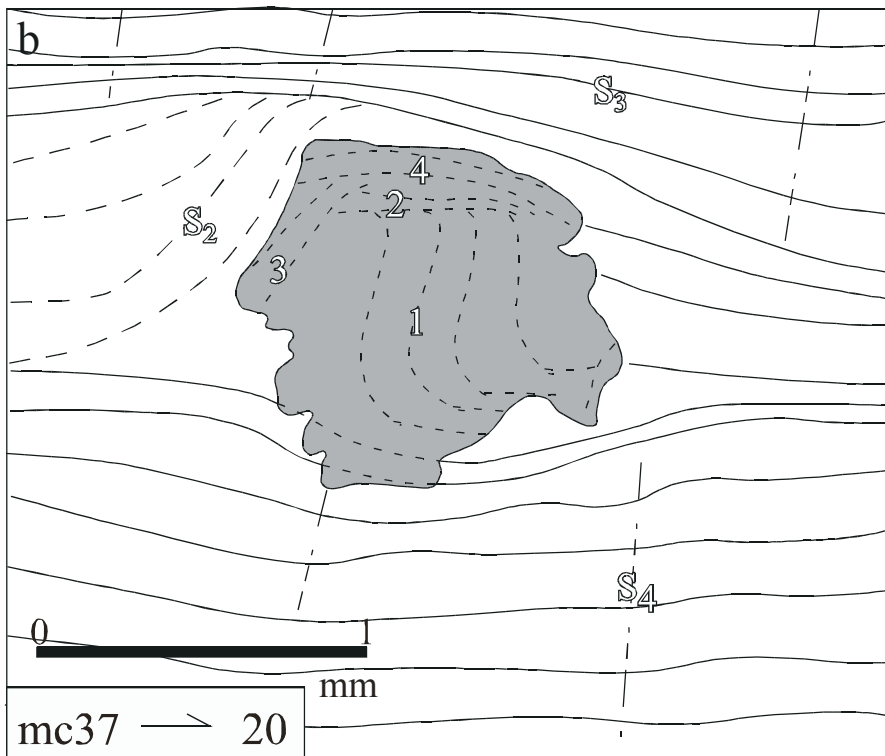
Figure 8. Photomicrograph from a vertical thin section shows a garnet porphyroblast with staircase inclusion trails (a). Interpreted line diagram (b) depicts a pre-existing foliation (1) and crenulation cleavage (2), respectively. S_2 is a steeply dipping foliation in biotite (bi) porphyroblast formed in the strain shadow of the garnet (grt) porphyroblast. S_3 is a gently dipping foliation intensified towards compositional layering.
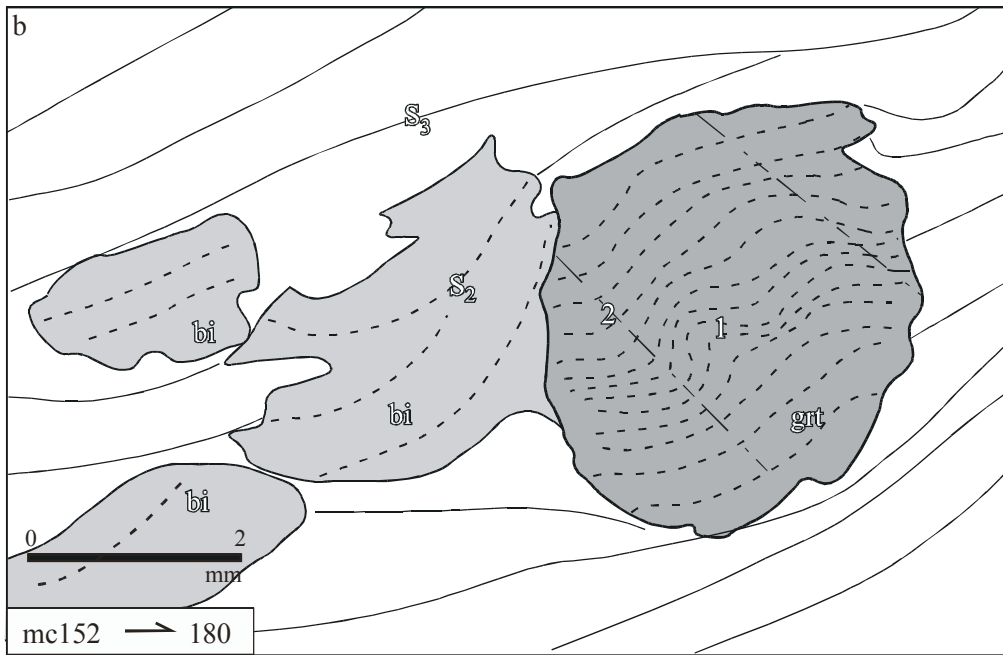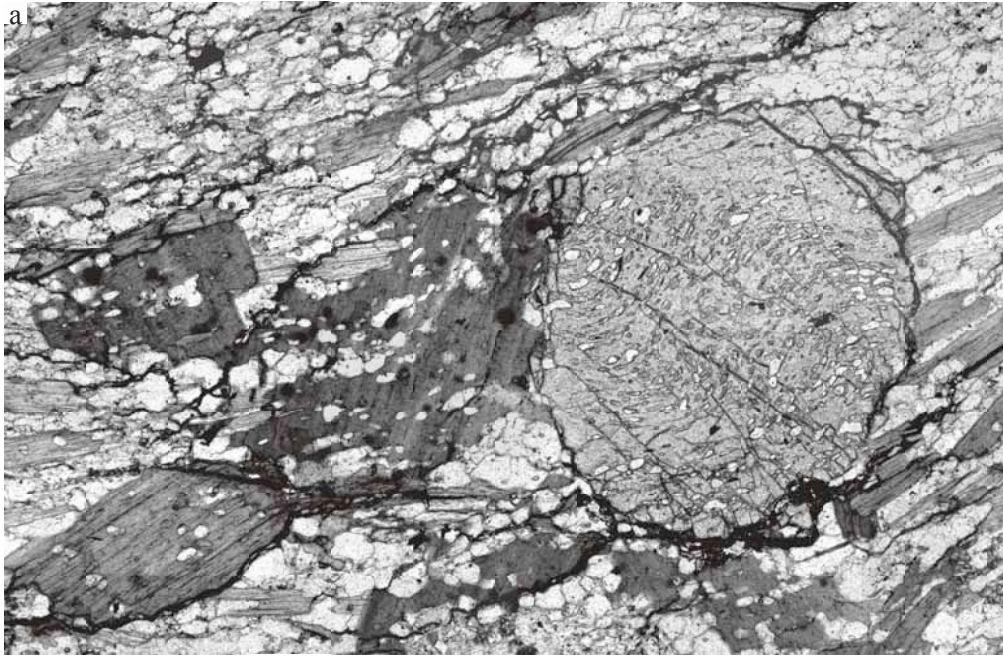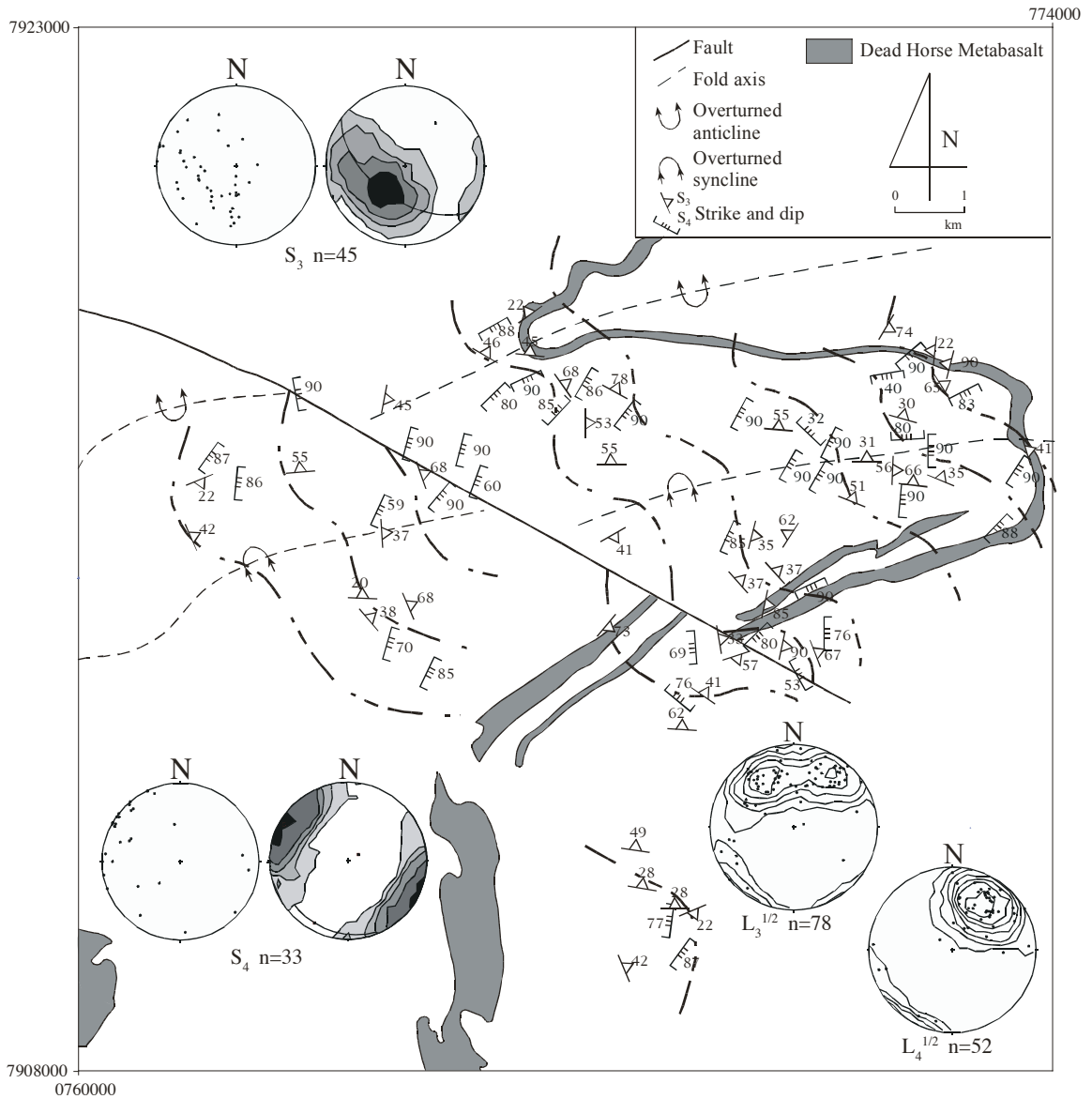
Figure 9. A structural map of S_3 and interpreted form-lines. Stereonet plot of S_3 suggests folding around a NE-SW axis. $L_3^{1/2}$ lineations are distributed in northern quadrants and $L_4^{1/2}$ lineations lie parallel to the axial plane of NE-SW folds (F_4).

Figure 10. A photo showing NE-SW trending folds (F_4) in which S_3 is parallel to compositional layering and S_4 appears as an axial plane. View is looking towards NNE.

Figure 11. Photomicrograph taken from a vertical thin section that shows garnet (grt) partially surrounded by a staurolite (st) porphyroblast with S_i continuous with the matrix (a). Interpreted line diagram (b) depicting sigmoidal inclusion trails within the core of a garnet porphyroblast represent gently dipping foliation (1) that is the hinge of the steeply dipping crenulation (2) in the rim. S_2 truncates the pre-matrix foliations exiting the garnet porphyroblast and it is also truncated by S_3, which is the dominant matrix foliation. S_4 is a steep weaker crenulation at the edge of the staurolite porphyroblast.

N   S
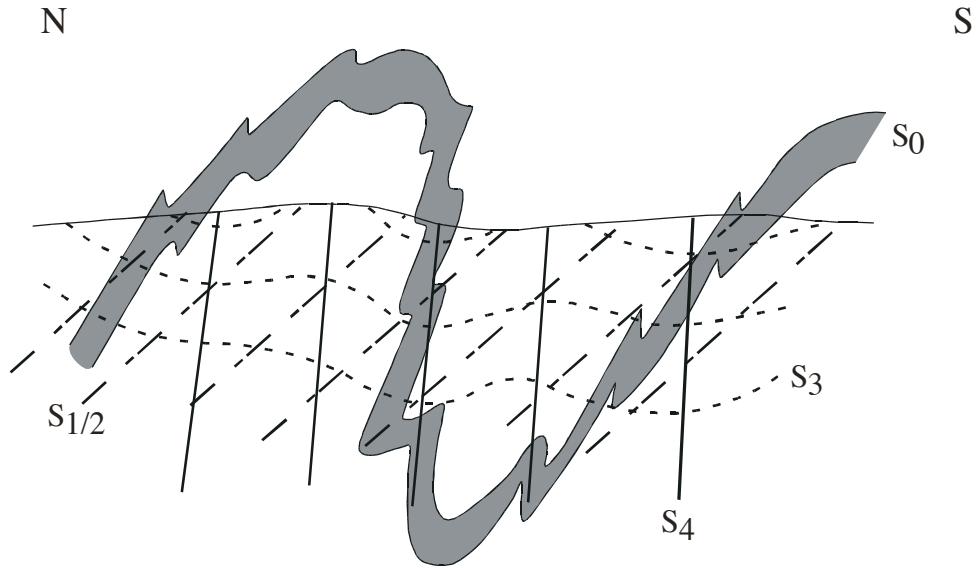
S_0

$S_{1/2}$

S_3

S_4
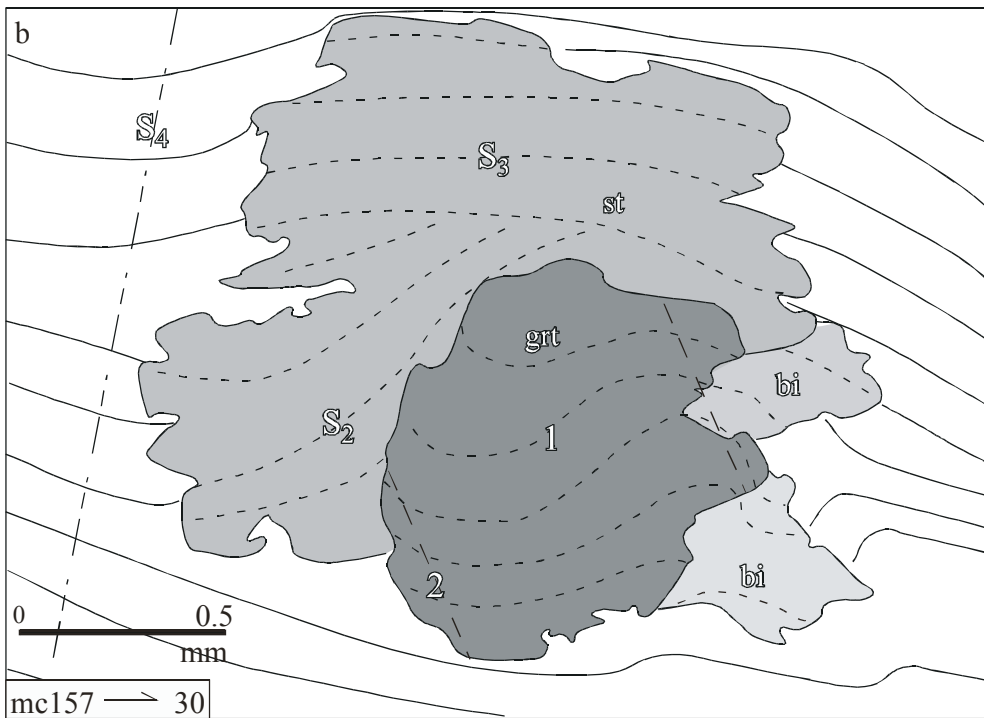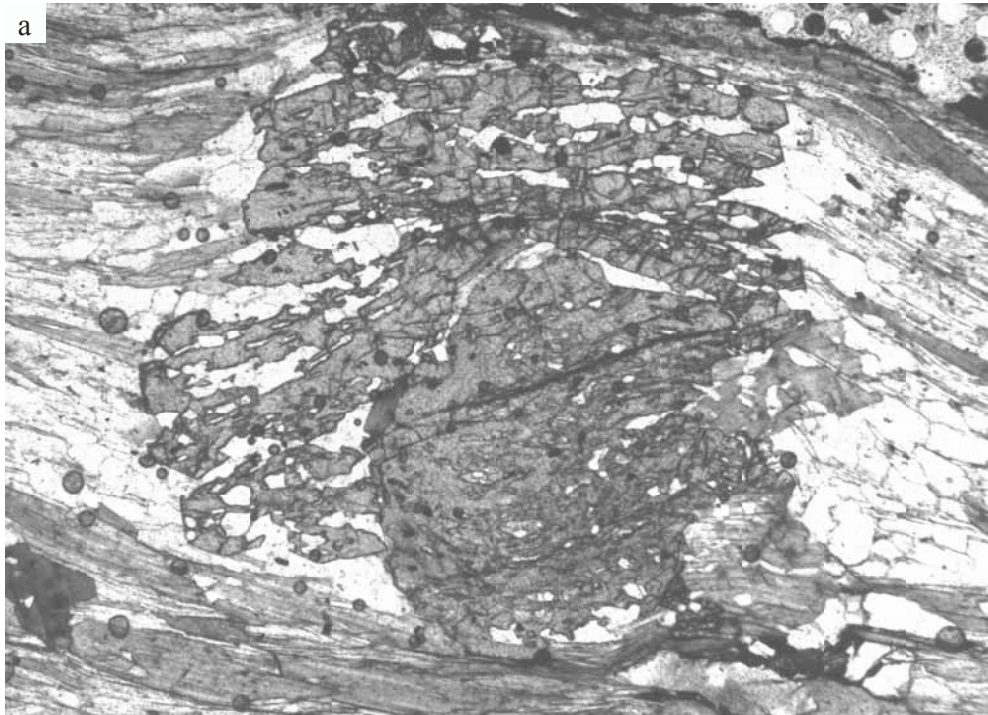
Figure 12. A simplified cross-section taken along a line A-A` in Fig. 2 shows the relationships of major structural features in the matrix.

Figure 13. Photomicrograph from a vertical thin section showing a garnet porphyroblast with spiral inclusion trails truncated by the matrix (a). Accompanying line diagram shows the interpretation of successively formed foliations (1-6), which were trapped as inclusions (b). Truncations of these foliations are visible between inclusion trails exiting the porphyroblast and matrix foliations S_1 and $S_{1/2}$.
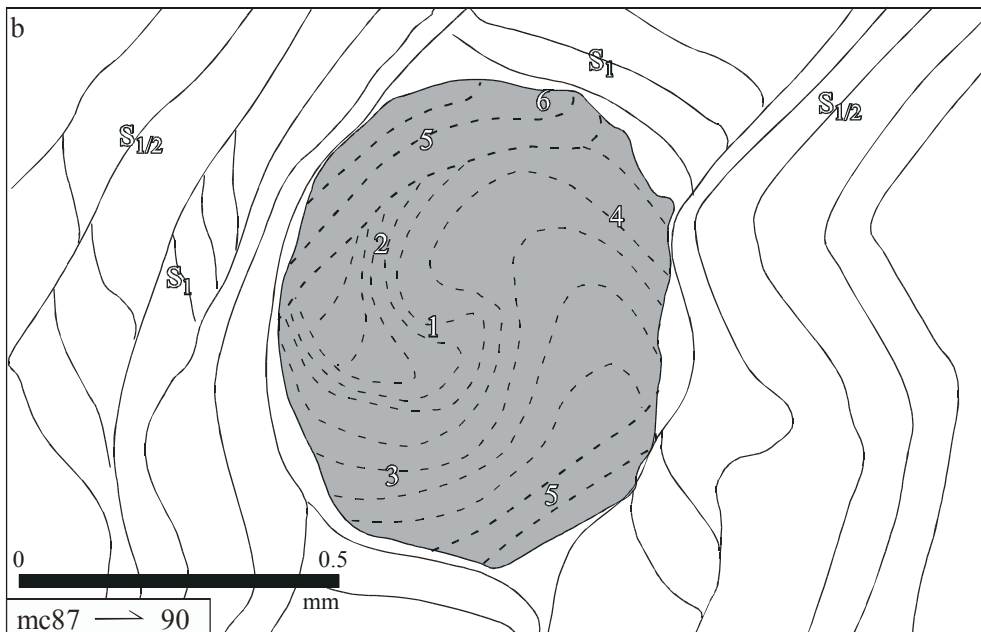
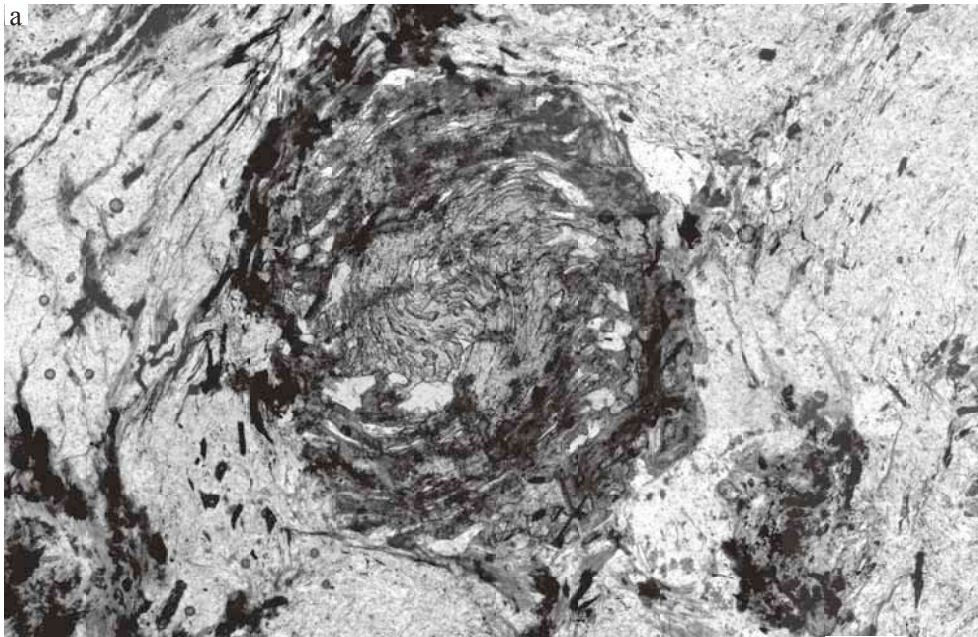Figure 14. Photomicrograph from a vertical thin section shows a staurolite porphyroblast preserving a differentiated crenulation cleavage as inclusions (a). Interpreted line diagram (b) shows the differentiated crenulation in which hinges represent gently dipping S_1 and long limb of the crenulations refers to steeply dipping pre-S_1, which is continuous with the matrix foliation $S_{1/2}$.
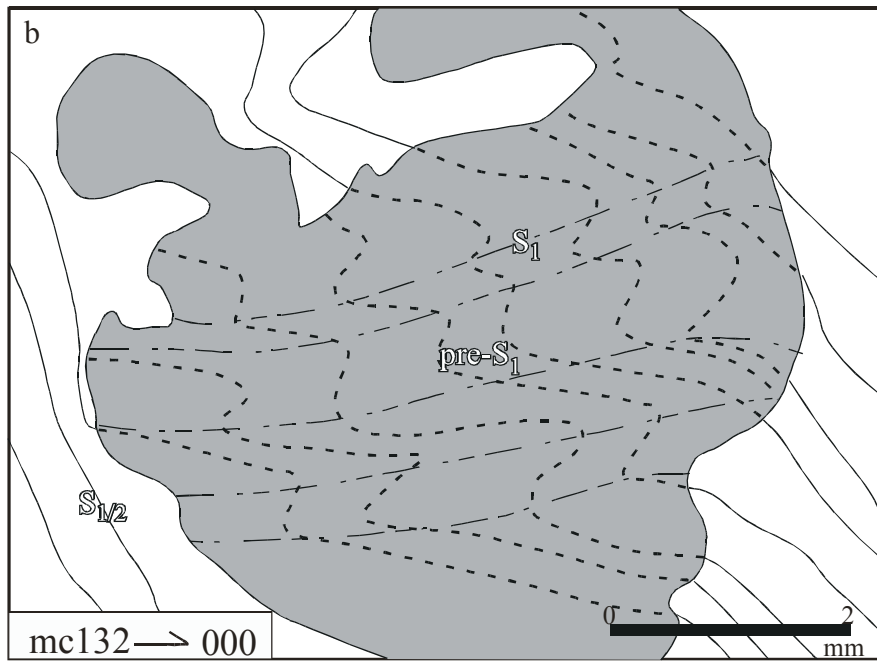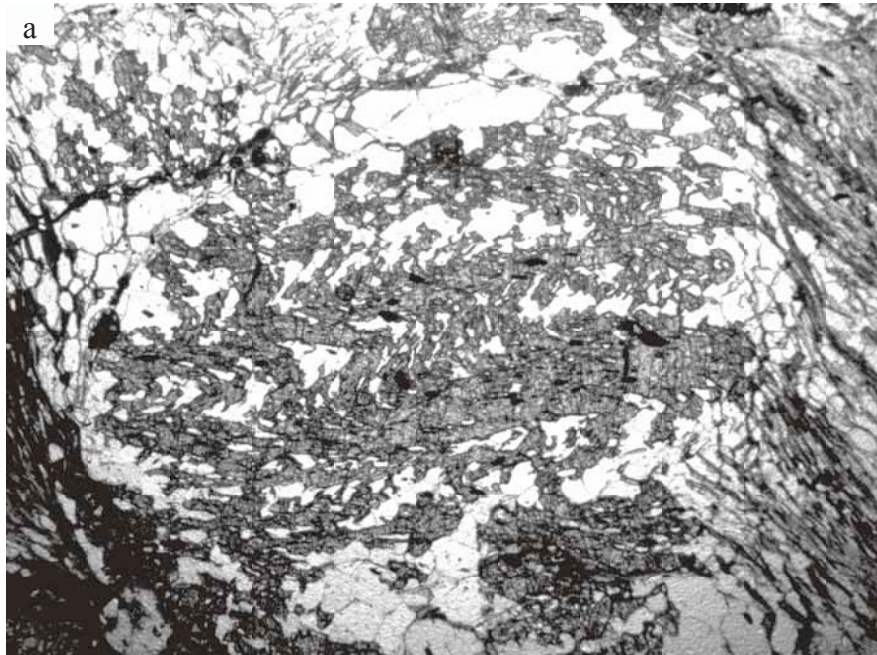
Figure 15. A map showing the distributions of FIA1 (ENE-WSW), FIA2 (E-W), FIA3 (N-S) and FIA4 (NE-SW) with respect to major structures across the study area.

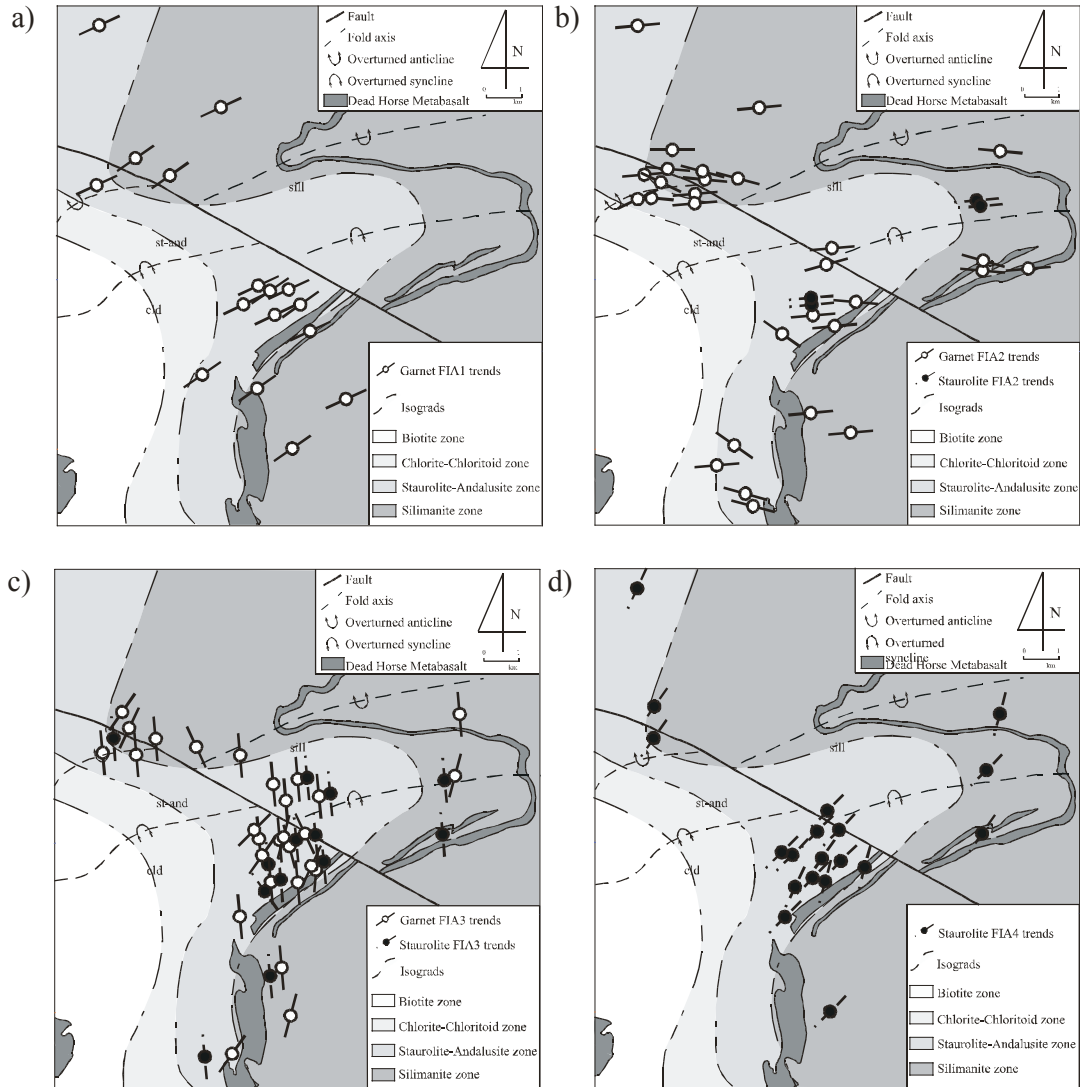| Sample Number	Garnet Core – Rim	Staurolite Core – Rim	Sample Number	Garnet Core – Rim	Staurolite Core – Rim
Mc1.1	105 -	175 -	Mc158	175 -	45 -
Mc1.2	105 -		Mc159	15 -	
Mc103	35		Mc160	75 -	45 -
Mc105	85 – 175		Mc17	95 – 175	15 -
Mc108	95 -		Mc2	105 -	
Mc110	155		Mc20		85 -
Mc12	85 -	175 -	Mc21		85 -
Mc121	35 -		Mc22		175 -
Mc130	55 -	175 –	Mc23	95 -	
Mc132A	85 -	15 -	Mc24	105 -	
Mc132B	65 -	175 -	Mc24.1	85 – 175	
Mc133	175 -	45 -	Mc25	105 -	
Mc134	145 -	25 -	Mc26	175 -	
Mc135	125 -		Mc27	175 -	
Mc137	85 -	175 -	Mc28	175 -	
Mc14.1	25 -	175 -	Mc3	125 -	
Mc14.2	95 -	15 -	Mc30	85 -	45 -
Mc140	65 -	85 -	Mc31	155 -	175 -
Mc15	5 -		Mc32	55 -	45 -
Mc151	85 -		Mc33	115 -	
Mc152	65 - 85	175 – 45	Mc34	25 -	
Mc153	95 -		Mc35.1	35 -	35 -
Mc154	55 -		Mc35.2	95 -	
Mc157	175 -	175 – 45	Mc36	65 – 85	
Mc37	85 – 175	45 -	Mc66	85 -	
Mc38	55 -		Mc68	105 -	175 -
Mc39	65 – 85	25 -	Mc7	15 -	45 -
Mc49	65 – 175		Mc71	85 -	
Mc5	55 – 15	175 – 45	Mc8	175 -	175 -
Mc55	85 -	15 - 45	Mc81	175 – 15	45 -
Mc58	65 -		Mc84	65 -	45 -
Mc6	95 -	35 -	Mc87	55 -	
Mc13	175-		Mc9	175 -	175 -
Mc65	65 -				

Table 1. A list of FIA measurements for each sample from core and rim of garnet and staurolite porphyroblasts.

a)

N=112   total FIA
Class int.=10°
Max per.=23.9

b)

N=74   garnet FIA
Class int.=10°
Max per.=19.4

c)

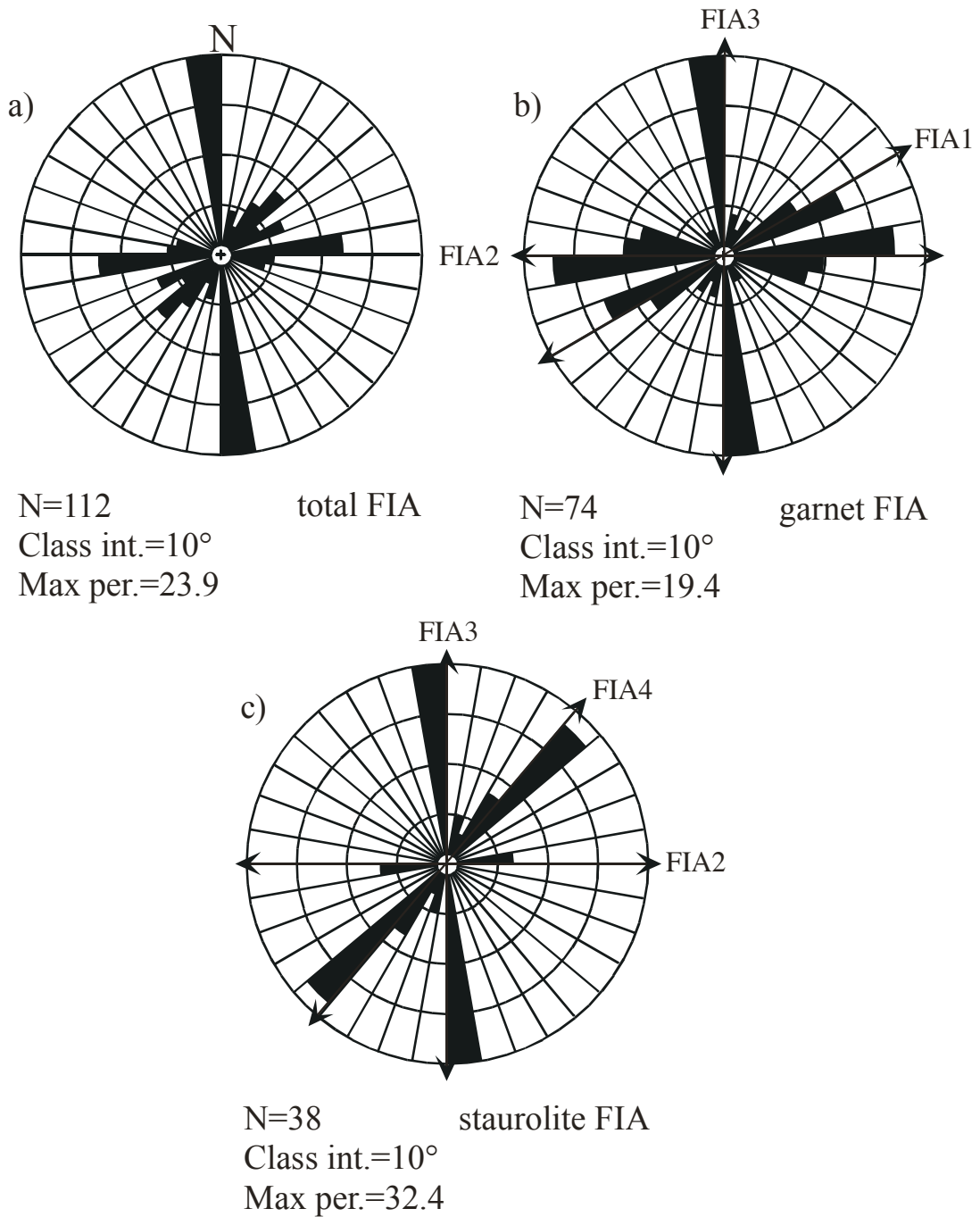N=38   staurolite FIA
Class int.=10°
Max per.=32.4

Figure 16. Rose diagrams showing the orientations of total FIAs (a), FIA1,

FIA2 and FIA3 in garnet porphyroblasts (b) and FIA2, FIA3 and FIA4 in

staurolite porphyroblasts (c) across the study area.

Figure 17. A sketch cross-section (a) across the folds including both the anticline and syncline in the area. Histograms (b, c, d) showing the distributions of asymmetries preserved in porphyroblasts formed around FIA1-FIA4 on the limbs of the folds divided as A, B, C. The S and Z shaped lines on the columns of histograms refer to asymmetries observed for FIAs with top to the left or right, and right side up or down shear senses.
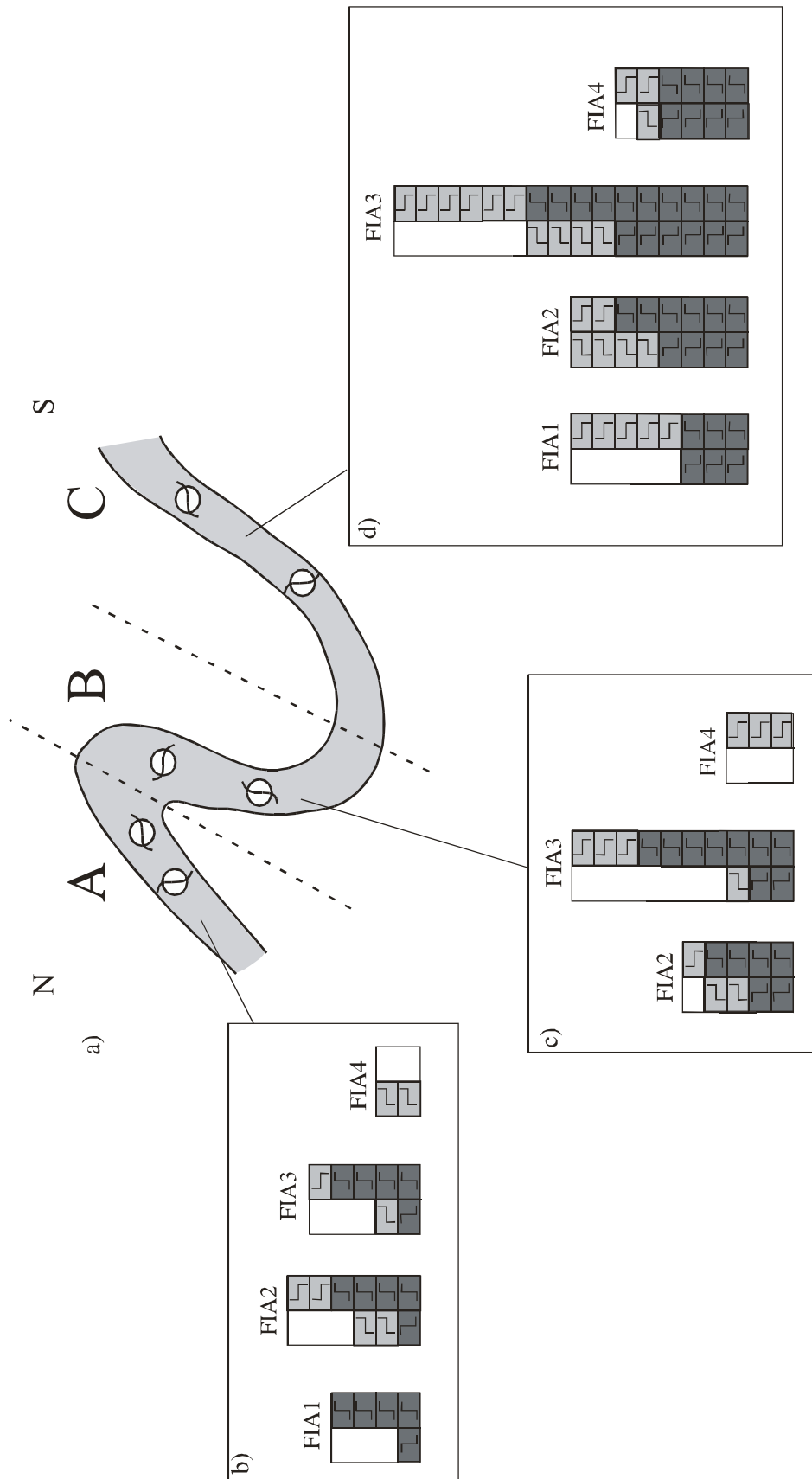
Figure 18. A sketch figure showing the stages of porphyroblast growth and the effect of deformation partitioning from one event to another. Microfracture development occurs soon after the deformation commenced (a). As deformation continues the microfracture density decreases (b), and porphyroblast growth ceases once a differentiated crenulation cleavage is formed and a consistent pattern of deformation partitioning is achieved (c). As the deformation intensifies, micas recrystallises along progressive shearing domains (d). During later stages of the same deformation, S_e is destroyed and S_i is rotated towards the compositional layering because of the reactivation, hence S_r dominates the matrix but in the strain shadow of the porphyroblast S_e remains as a relict foliation (e). In the next deformation event, deformation is repartitioned and porphyroblast growth continues in the new progressive shortening sites (f). At this stage, relict S_e trapped as inclusions in the rim and S_{e+1} is formed in the matrix. (Modified from Bell et al., 2004).

a)   b)

THE IMAGES ON THIS PAGE HAVE BEEN REMOVED DUE TO COPYRIGHT RESTRICTIONS

c)   d)

e)   f)